

Photodetachment photoelectron spectroscopy of multiply charged anions using electrospray ionization

Lai-Sheng Wang,^{a)} Chuan-Fan Ding, and Xue-Bin Wang

*Department of Physics, Washington State University, Richland, Washington 99352
and W. R. Wiley Environmental Molecular Sciences Laboratory, Pacific Northwest National Laboratory,
Richland, Washington 99352*

S. E. Barlow

*W. R. Wiley Environmental Molecular Sciences Laboratory, Pacific Northwest National Laboratory,
Richland, Washington 99352*

(Received 20 November 1998; accepted for publication 8 December 1998)

A magnetic-bottle time-of-flight (TOF) photoelectron spectrometer, coupled with an electrospray ionization source, has been developed for the investigation of multiply charged anions in the gas phase. Anions formed in the electrospray source are guided by a radio-frequency quadrupole ion guide into a quadrupole ion trap, where the ions are accumulated. A unique feature of this apparatus involves the coupling of a TOF mass spectrometer to the ion trap with perpendicular ion extraction. The ion trap significantly improves the duty cycle of the experiments and allows photodetachment experiments to be performed with low repetition-rate lasers (10–20 Hz). This novel combination makes the photodetachment photoelectron spectroscopy studies of multiply charged anions possible for the first time. Furthermore, the perpendicular extraction of ions, pulsed out of the ion trap, to the TOF mass spectrometer allows the ion energies to be conveniently referenced to ground, simplifying the configuration of the TOF mass spectrometer and the subsequent magnetic-bottle TOF photoelectron spectrometer. The mass resolution ($M/\Delta M$) achieved is about 800 for smaller ions. The magnetic-bottle photoelectron spectrometer resolution is about 11 meV full width at half maximum for 0.5 eV photoelectrons with an overall resolution of $\Delta E/E \sim 2\%$. The detailed design, construction, and operation of the new apparatus are presented. © 1999 American Institute of Physics. [S0034-6748(99)00804-7]

I. INTRODUCTION

Photoelectron spectroscopy (PES) is a powerful experimental technique to probe the electronic structure of matter.^{1,2} It has been widely used to study singly charged anions,^{3–10} providing electron affinities and information about low-lying excited electronic states for a vast number of neutral species and clusters. In this article, we describe a newly developed PES instrument designed to investigate multiply charged anions. Multiply charged anions are ubiquitous in nature and play prominent roles in chemistry, biology, and environmental and materials sciences. During the past three decades, although singly charged anions have been extensively studied,^{3–14} few studies have been carried out on multiply charged anions in the gas phase and very limited knowledge exists about them.^{14–16} This is partly due to the fact that many multiply charged anions are unstable in the gas phase, whereas they are stabilized in the condensed phase through solvation and electrostatic interaction with counterions. In the gas phase, these stabilizing factors are absent and the large Coulomb repulsion between two or more excess negative charges makes multiply charged anions very fragile to electron loss or fragmentation. Thus, the formation and characterization of multiply charged anions have been challenging both experimentally and theoretically.

Even if a multiply charged anion is stable in the gas phase, the Coulomb repulsion between the excess charges makes its formation through sequential electron attachment very difficult.¹⁶ Recently, the electrospray ionization (ESI) technique,^{17–19} which is widely used in biological mass spectrometry,²⁰ has been demonstrated to be a powerful technique to produce isolated multiply charged anions in the gas phase.^{21–25} Doubly charged anions were first observed using mass spectrometry in large organic molecules where the excess charges are well separated reducing the Coulomb repulsion.^{26–30} Recently, doubly charged anions have been observed for small carbon clusters,^{31,32} fullerenes,^{33–39} and anion–solvent complexes.^{21–25} Theoretical search of stable multiply charged anions has been very active lately, with a number of multiply charged anions predicted to be stable in the gas phase.^{15,40–45}

PES, in which photoemitted electrons from an anionic species by a fixed energy photon are measured, is an ideal technique to investigate the intrinsic properties of multiply charged anions in the gas phase. PES provides direct measurements of the excess electron binding energies in multiply charged anions, thus allowing information about their stability and intramolecular Coulomb repulsion to be obtained.

Our new PES instrument couples a magnetic-bottle time-of-flight (TOF) photoelectron analyzer and an ESI source, featuring a quadrupole ion trap to accumulate anion number

^{a)}Electronic mail: ls.wang@pnl.gov

densities and a TOF mass spectrometer (TOFMS). The novel design of the apparatus involves a low-energy unloading of the stored ions from the ion trap and a subsequent perpendicular extraction of the ions for TOF mass analyses. The perpendicular ion extraction decouples the ion trap and the TOFMS operation. This decoupling allows the ion-beam energies to be conveniently referenced to ground and at the same time allows reasonable mass resolution to be achieved in a simple linear TOFMS design. A radio-frequency (RF) quadrupole ion guide is used to enhance the ion transmission from the ESI source to the ion trap and is also essential for the successful operation of the new apparatus.

The detailed design, construction, and operation of the apparatus are reported in the current article, which is organized as follows. In Sec. II, we discuss the general considerations of our design and choices of techniques. The details of the apparatus are described in Sec. III, followed by a presentation of the experimental procedures and performance in Sec. IV. Finally, a discussion and perspective is given.

II. GENERAL CONSIDERATIONS

A. Electrospray as an ion source for free multiply charged anions

The challenge in performing PES experiments on multiply charged anions is to find a general ion source that is capable of producing a stable beam (either pulsed or continuous) of a given anion species. That has been a difficult task because even if a multiply charged anion is stable in the isolated form, the Coulomb repulsion between the excess charges makes it very difficult for its formation in the gas phase through sequential electron attachment. For example, both C_{60}^{-2} and $Cr_2O_7^{-2}$ are known to be stable (long lived) in the isolated form.^{22,34,35} We have produced and studied the singly charged versions of these species using a laser vaporization cluster source.^{6,46} However, their doubly charged anions have not been successfully produced with the laser vaporization technique despite repeated attempts. The experimental techniques used to produce multiply charged anions have been previously reviewed.¹⁶ Recently, it has been shown that the ESI technique can produce multiply charged anions easily from a solution sample.^{21–25} In the ESI source,^{17–19} a liquid solution containing the desired anions is sprayed through a small needle under high voltage (the polarity of the bias determines the signs of the charged species produced), generating highly charged fine liquid droplets. The breakup of these charged droplets and the subsequent desolvation produce singly or multiply charged species that exist in the solution. The ESI technique has been used to produce a number of multiply charged ions in the gas phase.^{21–25} Therefore, ESI appeared to be the most promising technique to produce multiply charged anions in the gas phase for our interested PES experiments.

B. Choice of the magnetic-bottle TOFPES technique

The ESI source is intrinsically continuous, so the natural choice for the photoelectron spectrometer would appear to be the hemispherical analyzer, which has been used very successfully in anion PES experiments.^{4,5,7} However, there are

two potential drawbacks. First, the hemispherical analyzer scans the kinetic energy and is quite time consuming to measure a PES spectrum. It requires an intense and very stable ion source in order to collect a spectrum within a reasonable amount of time. Second, and more importantly, cw laser sources are limited, in particular in the ultraviolet (UV) and vacuum ultraviolet (VUV) energy ranges, putting serious limitations on the possible experiments. On the other hand, TOFPES techniques are more convenient and have several advantages. First, they are more compatible with the available pulsed laser sources, particularly in the UV and VUV energy ranges. Second, in TOF techniques the whole PES spectrum is taken at each laser shot, thus putting less stringent requirements on the ion-beam stability. Third, the magnetic-bottle TOFPES technique can be employed, which gives nearly 100% electron collection efficiency. The high efficiency of this angle-integrated technique allows even weakly populated anion species to be studied.

The magnetic-bottle photoelectron analyzer was first described in detail by Kriut and Reed as a high collecting efficiency photoelectron spectrometer and photoelectron-image magnifier.⁴⁷ They demonstrated the performance of this device using multiphoton ionization of xenon in a 1 T homogeneous magnetic field. In this configuration, they were able to collect electrons from 2π sr (50% collecting efficiency). The magnetic-bottle analyzer was later reconfigured to study size-selected anions with pulsed cluster beams by two groups,^{9,48} who performed photodetachment in a diverging magnetic field such that electrons from nearly 4π sr could be collected. However, these early designs gave rather poor energy resolutions. The resolution of the 4π configuration was later improved significantly for studies of size-selected clusters.^{6,49,50} The key improvements in our previous design were to fully decelerate the anions prior to photodetachment using a momentum decelerator and to replace the electromagnet (solenoid) with a permanent magnet machined to a special shape.^{6,50} It has thus become a highly versatile and efficient technique for the studies of size-selected anions and is our natural choice for the multiply charged anion experiments.

C. Continuous-to-pulsed operation: Quadrupole storage TOF mass spectrometry with perpendicular ion extraction

The ESI source is inherently continuous whereas both the TOFMS and TOFPES are pulsed operations. Several groups have already designed ESI sources coupled with TOF mass spectrometry for biomolecular mass analyses.^{51–55} Other continuous sources have also been coupled with TOFMS, taking advantage of the fast data acquisition speed of the TOF operation.^{56,57} In all these designs, a high repetition rate ranging from one to several kHz was used to enhance the experimental duty cycle. Typically, a few ions per pulse were counted, but a high total count rate was achieved due to the high repetition rates. Although this mode of operation is perfectly suitable for mass spectrometric experiments, it is not particularly ideal for PES experiments. Low repetition rate operation is more advantageous for PES ex-

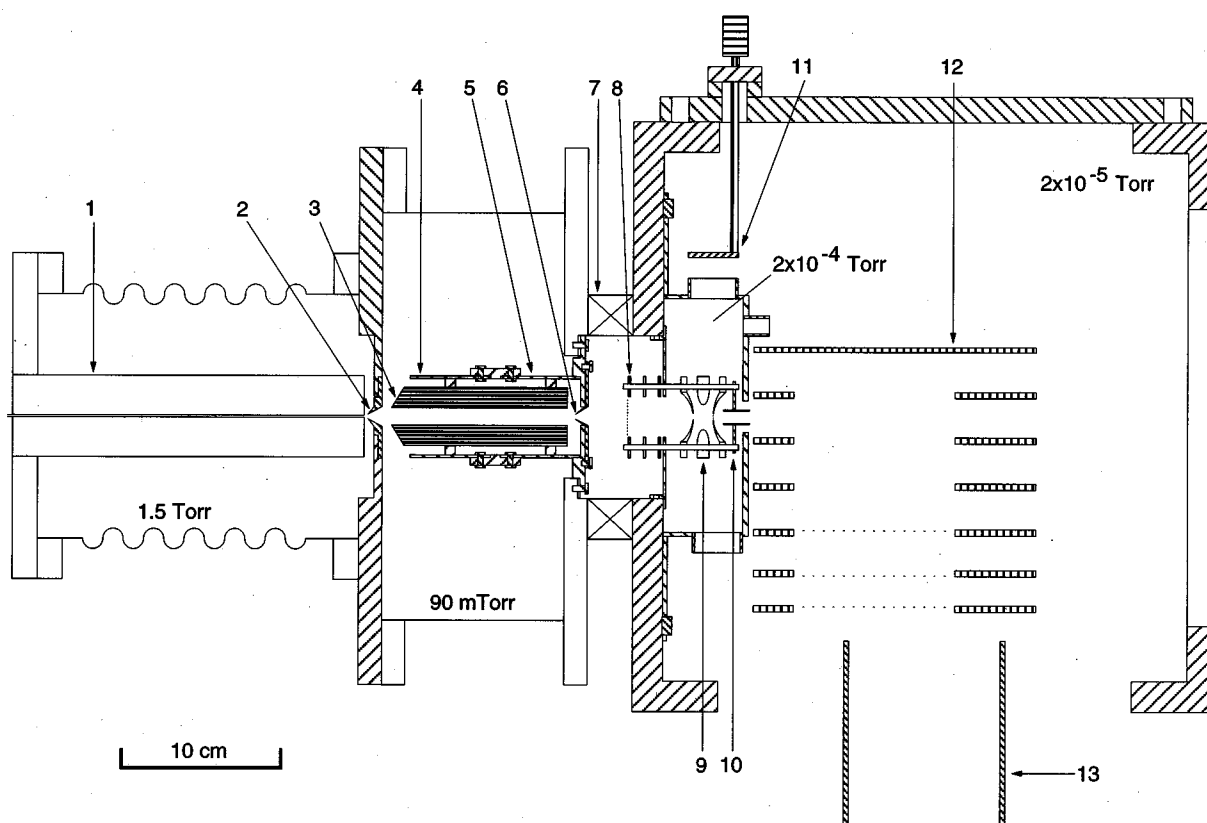


FIG. 1. Schematic diagram of the electrospray ionization source for multiply charged anions: (1) heated desolvation capillary assembly; (2) the first skimmer (1.5 mm diam); (3) radio-frequency quadrupole ion guide; (4) the first stainless-steel tube shielding (biased at +10 V); (5) the second stainless-steel tube shielding (biased at +50 V); (6) the second skimmer (1.5 mm diam); (7) gate valve; (8) ion trap entrance lens assembly (a 90% open area grid is mounted on the first electrode, which is biased at +80 V); (9) quadrupole ion trap; (10) stainless-steel tube lens (8 mm i.d.); (11) adjustable cap controlling the conductance and pressure of the ion trap region; (12) time-of-flight mass spectrometer extraction stack; and (13) horizontal ion-beam deflector.

periments for two reasons: (1) low repetition rate lasers are more readily available; and (2) the mass selection and ion deceleration could be more conveniently accomplished in this mode. However, in this mode the duty cycle is extremely low. For example, assuming the repetition rate of the detachment laser is at 100 Hz and an effective ion collecting duration of 10 μ s, we would still only obtain a duty cycle of 10^{-3} .

A convenient solution to this problem is to use storage mass spectrometry.⁵⁸ A quadrupole ion trap can be inserted in the beam path to accumulate ions. The ions can be stored for a specified period of time and then pulsed out as an ion packet for subsequent TOF mass analyses. Quadrupole ion traps have been gaining popularity as a sensitive mass spectrometric technique.⁵⁸ Several groups have already used the quadrupole ion traps coupled with TOFMS for biomolecular mass spectrometry^{59–61} and for trace element analyses.^{62,63} However, in all the previous designs of ion storage/TOFMS, the ions are extracted from the ion traps at high voltages and the TOFMS is collinear with the ion trap. The advantage in this mode is that the ions are extracted from the trap as a well-defined ion packet, conducive to the subsequent TOF analyses. However, upon exiting the trap the ions are further accelerated to high kinetic energies and cannot be referenced to ground, i.e., the TOF path has to be floated at a high potential. This in turn makes subsequent manipulation of the ion beam difficult. Therefore, in our new apparatus, we un-

load the stored ion packet at low kinetic energy and use perpendicular ion extraction for the subsequent TOFMS analyses. This mode essentially decouples the ion trap operation and the TOFMS, allowing us to reference the ion beam to ground potential by using pulsed ion extraction for the TOFMS and simplifying the mass selection, deceleration, and PES operation. As will be described below, a special ion lens is needed to focus and guide the low-energy ion beams exiting the ion trap for the successful operation of this mode.

III. APPARATUS DESCRIPTION

Figure 1 shows the details of the ESI source and TOFMS extraction region and Fig. 2 shows a schematic diagram of the whole experimental apparatus. The apparatus can be divided into three major sections: (I) ion source; (II) TOF mass spectrometer; and (III) magnetic-bottle PES analyzer. Charged liquid droplets from a syringe needle enter the desolvation capillary (1). Molecular ions exiting the desolvation capillary are guided into the quadrupole ion trap (9) through a RF-only quadrupole ion guide (3) and an entrance focusing lens system (8). Ions pulsed out of the ion trap are guided and focused by a tube lens (10) into the extraction zone (12) of the TOF mass spectrometer, where ions are extracted perpendicularly. The extracted ions in the TOFMS flight tube are focused by two Einzel lens systems (14 and 19), mass selected, and decelerated (23) before entering the detachment

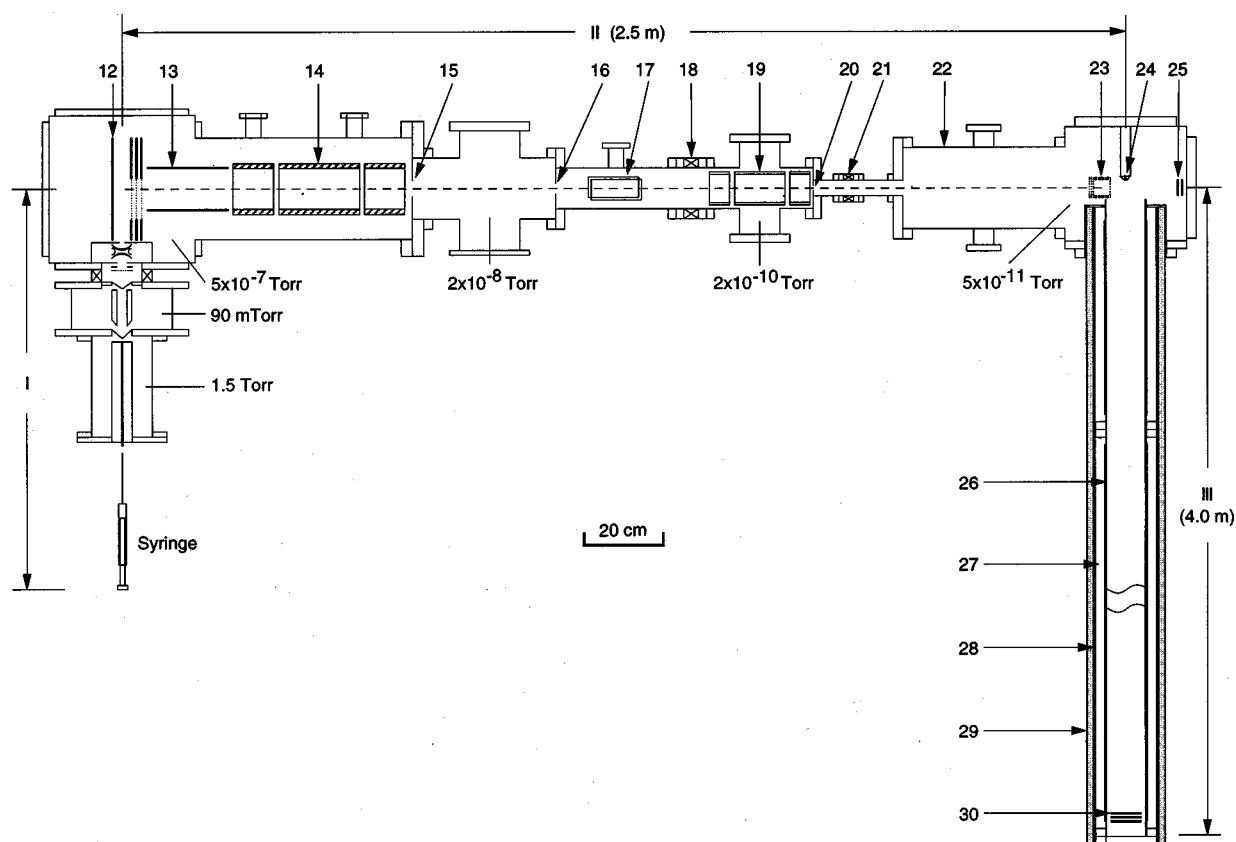


FIG. 2. Schematic diagram of the electro spray ionization-time-of-flight magnetic-bottle photoelectron spectroscopy facility. (I) Electro spray ionization source (see Fig. 1). (II) Time-of-flight mass spectrometer: (12) time-of-flight mass spectrometer (TOFMS) extraction stack (see Fig. 1); (13) horizontal ion-beam deflector (see Fig. 1); (14) the first TOFMS Einzel lens assembly; (15) the first TOFMS aperture (38 mm i.d.); (16) the second TOFMS aperture (25 mm); (17) vertical ion-beam deflector; (18) gate valve; (19) the second TOFMS Einzel lens assembly; (20) the third TOFMS aperture (13 mm i.d.); (21) gate valve; (22) 20 cm i.d. large vacuum chamber; (23) three-grid mass gate and momentum decelerator assembly; (24) permanent magnet (NdFeB ceramic magnet); (25) 40 mm i.d. dual microchannel plate (MCP) in-line ion detector; (26) baking heaters; (27) heat insulation; (28) low-field solenoid; (29) double layer μ -metal shielding; and (30) 18 mm z -stack fast MCP photoelectron detector.

zone of the magnetic-bottle PES analyzer. A fixed wavelength laser beam (perpendicular to the figure) is crossed with the ion beam in the detachment zone. Photoelectrons emitted in all 4π solid angles are collected by the magnetic bottle, formed by a permanent magnet (24) and a low-field solenoid (28), which guides the electrons to the detector (30). Details are described in the following.

A. Electro spray and desolvation capillary

A quartz syringe with a stainless-steel needle is used for the electro spray. The sample solution is actually sprayed into the ambient atmosphere through a 4 cm long fused silica needle (0.01–0.001 mm diam), which is connected at the end of the stainless-steel syringe needle. The stainless-steel needle is biased at -1.9 to -2.5 kV for the formation of negatively charged liquid droplets. A microprocessor-controlled syringe pump (World Precision Instrument SP100i) is used to deliver the solution. The highly charged liquid droplets formed from the quartz needle are fed into the heated desolvation capillary assembly (1), consisting of a 0.8 mm i.d. stainless-steel tube (20 cm long) tightly fit into a copper block (20 cm long, 3.4 cm o.d.). The copper block is heated by two heaters inserted through two drilled holes (7.5 cm deep, 0.7 cm diam). The heated copper block is in turn

inserted into a thermally insulating shroud, which is mounded and sealed to the end flange. The temperature of the desolvation capillary, ranging from 50 to 100 °C, is measured by a thermal couple and controlled by a transformer. The end flange is attached to a bellows so that the whole desolvation assembly can be positioned in the x - y - z directions. The first vacuum chamber defined by the bellows is pumped by a 10 l/s mechanical pump to a pressure of approximately 1.5 Torr during experiments with the 0.8 mm i.d. capillary.

B. RF-only quadrupole ion guide

The charged liquid droplets are broken down and desolvated in the heated desolvation capillary (1), converting the ionic species present in the solution sample into the gas phase.⁶⁴ The mechanisms of the ion formation have been discussed previously.²⁰ The ionic species emerging from the desolvation capillary pass through a 1.5 mm diam skimmer (2) at thermal energies and enter the second differentially pumped chamber, evacuated by a 180 l/s blower pump to about 80–100 mTorr. The distance between the heated desolvation capillary and the skimmer is kept at about 3 mm, typically, and is adjustable through the bellows.

At the low vacuum of the second chamber (80–100 mTorr), the mean-free paths of ions are less than the dimen-

sions of the vacuum chamber. Hence, electrostatic ion optics are no longer effective to focus and transmit the ions because of collisions with the background gases. RF-only quadrupole is a powerful ion transmission technique in the lower vacuum regime, typically, from 1 to 100 mTorr. It has been reported that the ion transmission efficiency of a RF-only ion guide could be as high as 90% due to a collisional focusing effect.⁶⁵

A RF-only quadrupole ion guide is used in our apparatus as an ion focus and transmission device (3). Our system was made of four 10 cm long and 2.5 cm diam stainless-steel rods (3). We have two RF power supplies with output frequencies centered around 1.6 and 1.0 MHz, corresponding to two mass ranges (M/Z): approximately 50–1000 and 70–2500, respectively. The mass range can be increased by using a set of smaller quadrupole rods. Two stainless-steel cups (4 and 5) are used to shield the high-frequency RF field and can be biased to optimize the transmission efficiency, which is typically 60% in our case.

C. Quadrupole ion trap

The guided ion beam passes through a second skimmer (6, 1.5 mm diam) into a third vacuum region, containing the quadrupole ion trap (9) and the ion entrance optics (8). This vacuum region is not separately pumped and the vacuum is controlled to about 0.2 mTorr by controlling the conductance (11) to the main ion extraction chamber, which is evacuated by a 2000 l/s diffusion pump (DP) to about 2×10^{-5} Torr. There is a flat vacuum gate valve (7) between the second and third chamber, isolating the high vacuum region.

The ion trap is a commercial device from the R. M. Jordan Company (Grass Valley, CA). There is a 3 mm diam hole on each of the two end caps, allowing ions to enter and exit the trap. The principles of the quadrupole ion trap have been well documented.⁵⁸ Its operation requires a background gas of about 10^{-4} – 10^{-5} Torr, so that ions can be confined to the center of the trap through collisional focusing. Helium is typically used as the background gas. Since we do not have a separate vacuum pump currently for the ion trap region, our background gases mainly consist of air and solvent molecules. With the current geometry and RF power supply (5 kV RF amplitude and 1 MHz frequency), the upper mass range (M/Z) of our ion trap is about 5000.

Since the ions exiting the second skimmer (6) are divergent and have low kinetic energies (~ 1 eV), we use an entrance lens system (8) to focus the ion beam into the trap. The first plate of this lens system is made of a 90% open area grid and biased at 80 V to extract the ions from the skimmer. The bias voltages at the second and third plates of this lens system are, typically, at 2 and 7 V, respectively, giving an entrance kinetic energy of about 4 eV for the ions. Under these conditions, we can achieve a total transmission of about 10% from the exit of the first skimmer to the entrance of the ion trap. Typical total ion current at the exit of the first skimmer is about 500 pA, resulting in about 50 pA total current at the entrance of the ion trap.

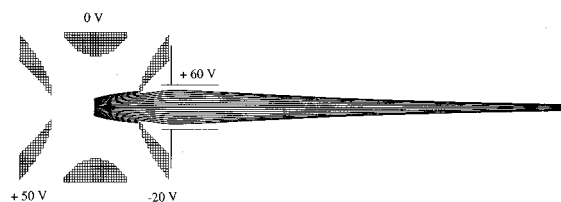


FIG. 3. Trajectory simulation for the low-energy unloading of stored ions from the ion trap using SIMION 3D. An 8 mm stainless-steel tube lens is placed just after the exit end cap and biased to focus and guide ions to the ion acceleration region of the TOFMS (see Fig. 1). The optimized potential for each electrode is shown, giving an average kinetic energy of ~ 10 eV for anions exiting the trap.

D. Unloading the ion trap and ion refocusing

One of the novel features of the current apparatus is the perpendicular coupling of the TOFMS to the ion trap, allowing decoupling of the operation of the ion trap and the TOFMS. The accumulated anions in the trap are gently pushed out at low kinetic energies. Since the ions are extracted perpendicularly for the subsequent TOF mass analyses, it is essential to unload the ions from the trap at as low kinetic energies as possible. However, the ion beam would diverge too much on its way to the TOFMS ion extraction region (12). We found a simple solution to the ion-beam divergence problem by simply adding a tube lens right after the trap (10). Through SIMION simulations, we found that the low-energy ion beam can be refocused into the TOFMS extraction zone by applying appropriate potentials to the two end caps and the tube lens. A SIMION simulation of the ion trajectory is shown in Fig. 3 with the optimum voltages. The tube lens was made of a 1.3 cm long and 8 mm i.d. stainless-steel tube and is biased at 60 V. Under these conditions, the kinetic energy of the anions exiting the trap is only about 10 eV, suitable for the perpendicular ion extraction. However, we did find that an ion deflector is needed to correct the ion-beam trajectory in the TOFMS flight tube and that the kinetic energies of the ions exiting the trap have a significant effect on the TOFMS resolution, as will be described below.

E. TOF mass spectrometer

As shown in Fig. 1, our TOFMS uses a modified Wiley–McLaren arrangement,⁶⁶ which was first described by de Heer and Milani.⁶⁷ The major modification involves an addition of a short free-flight zone in between the two acceleration stages of the original Wiley–McLaren design. This modification allows high mass resolution with a large extraction zone. We have previously described such a design with our laser vaporization cluster source.^{6,50} Even though the ion beam exiting the ion trap is focused by the tube lens, it can still exhibit a considerable spread in the direction of the beam path (perpendicular to the TOF extraction direction). Therefore, a large extraction zone is still required.

The anions are extracted perpendicularly with a high-voltage pulse (-1.25 kV). A horizontal deflector (13) is used to correct for the 10 eV transverse ion energy. An Einzel lens focuses the ion beam through the first differential pumping aperture (15). The ion extraction chamber is evacuated by a

2000 l/s DP to a base pressure of 5×10^{-7} Torr. The ion beam passes through the second TOFMS differential pumping chamber (base pressure, 2×10^{-8} Torr), which is pumped by a 1200 l/s DP. After passing a second aperture (16), the ion beam is refocused by a second Einzel lens (19) onto a set of in-line microchannel plate (MCP) detectors (24) in the electron detachment chamber. The ion beam can be steered by a vertical deflector (17) before entering the second Einzel lens. A third aperture (20) defines the third differential pumping zone, evacuated by a 200 l/s turbo molecular pump to a base pressure of 2×10^{-10} Torr. The total flight path of the TOFMS is 2.5 m long. A large vacuum chamber with a set of view ports (22) is attached to the detachment chamber to make room for future photofragmentation experiments. The detachment chamber is pumped by a cryopump (CTI Cryo-Torr 8, 4000 l/s) to a base pressure of 5×10^{-11} Torr. The pressures in all the four differential pumping regions of the TOFMS increase by about two orders of magnitude during the experiments.

F. Magnetic-bottle PES analyzer

There are several ways to design the magnetic bottle. One can use either a solenoid or a permanent magnet to produce the strong magnetic field. Theoretically, both the magnetic-field intensity and the shape of the magnet affect the electron energy resolution. According to our previous experience,⁵⁰ a permanent magnet with a 60° or 90° tapered angle and a sharp tip could give about 20 meV [full width at half maximum (FWHM)] energy resolution for 0.8 eV electrons.

As shown in Fig. 2, the configuration of our new magnetic-bottle TOFPES is similar to our previous design. The key to improving the resolution was to decelerate the anions to very low kinetic energies in order to eliminate the Doppler broadening. We used a momentum deceleration technique, which can effectively decelerate the anions to very low energies and at the same time reduce the initial beam energy spread. The three-grid mass gate and the momentum decelerator used in our new apparatus (23) is similar to our previous design.^{6,50} Several modifications have been made to further improve the energy resolution in our new apparatus. To minimize the effect of residual electric fields, we installed a stainless-steel shroud (not shown in Fig. 2) to shield the photodetachment zone and the magnetic-bottle area. The permanent magnet (24) is now mounted on a translation stage so that the position for the best resolution can be easily found. Furthermore, the position of the new magnet now can be adjusted to minimize the photoelectron noises at high photon energies. The total field-free electron flight tube is 4 m long. The whole detachment chamber and the TOF tube can be baked *in situ* up to 100°C to ultrahigh vacuum (5×10^{-11} Torr). The heaters (26), thermal shielding (27), low-field solenoid (28), and μ -metal shielding (29) are shown in Fig. 2. The electron detector (30) is a fast z stack consisting of a set of three MCPs.

IV. PERFORMANCE

A. Experimental procedure and timing sequence

Our experiments start from the electrospray, where a microprocessor-controlled syringe pump (World Precision Instruments SP100i) is used to deliver the liquid samples which contain the desired anions through a 0.01 mm i.d. fused silica capillary directly to the ambient atmosphere at room temperature. The capillary is biased at -1.9 to -2.5 kV through a stainless-steel needle to which the fused silica capillary is connected. The solution delivery rate is, typically, 50 ml/h. The concentration of the solution used is usually $\sim 10^{-4}$ M and the solvent is a mixture of 98% methanol and 2% water for producing isolated multiply charged anions. The solvent, pH, and solution concentration can all be changed to optimize the abundance of a given anion species. The desolvation capillary is heated to 50 – 100°C depending on the anions desired—bare anions require a higher desolvation temperature whereas a lower temperature is desirable for making solvated species. The desolvation capillary (1) and the first skimmer (2) are grounded at all time. The RF voltage is adjusted to optimize the transmission of a given mass range. The second skimmer (6) is biased at 1–4 V for all anions.

The ion beam is focused by a set of lenses (8) into the ion trap through a 3 mm diam hole on the entrance end cap. During the period of ion accumulation, both end caps are held at ground potential while a RF potential is applied to the central ring electrode. The RF frequency (1.0 MHz) is fixed and the RF voltage (0–5 kV) is varied to optimize a given mass range. After a predetermined trapping period (determined by the experimental repetition rate, usually 0.1 s at 10 Hz repetition rate), the RF voltage is turned off for a period of about $100 \mu\text{s}$ for the unloading of the stored ions. The timing sequence of the experiment is generated by three digital delay generators (DG535, Stanford Research Systems) and controlled by a PC. The schematic timing diagram of the experimental cycle is shown in Fig. 4. T_1 corresponds to the trapping time (0.1 s) relative to the start of the experimental cycle. A delay period (T_2) of about $1.5 \mu\text{s}$ is necessary to allow the RF to damp to near-ground potential before applying potentials to the end caps for the unloading. This delay period cannot be too long because otherwise the trapped anions will begin to diffuse from the center of the trap, decreasing the unloading efficiency. The $1.5 \mu\text{s}$ delay time is carefully chosen according to experimental measurements. After this delay period, a -50 V pulse is applied to the entrance end cap and a $+20$ V pulse is applied simultaneously to the exit end cap for $20 \mu\text{s}$ to gently push the trapped ions to the extraction region of the TOFMS (12).

After another delay period (T_3), a -1.25 kV high-voltage pulse is applied to the ion acceleration plates for about $100 \mu\text{s}$ to extract the ions perpendicularly into the TOFMS flight tube. T_3 is varied to optimize a given mass range because the ion beam exiting the trap tends to spread out along the beam axis. The anion beam is deflected, focused, and collimated down the 2.5 m long field-free flight tube. Mass spectra are taken by digitizing the MCP output of the in-line detector (25) using a transient digitizer (model

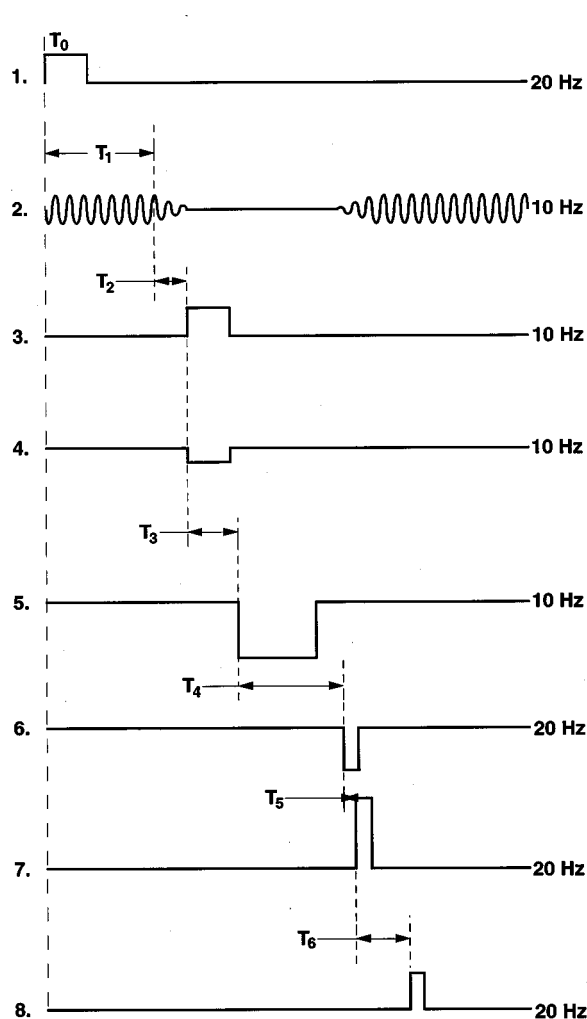


FIG. 4. Experimental timing sequence: (1) starting pulse of a whole experimental cycle; (2) ion trapping period (RF on, $T_1 \sim 0.1$ s) and ion unloading period (RF off, ~ 100 μ s); (3) unloading potential (+50 V) for the ion trap entrance end cap (T_2 , delay from ion trap RF off, ~ 1.5 μ s); (4) unloading potential (-20 V) for the ion trap exit end cap; (5) perpendicular ion extraction pulse for TOFMS (-1.25 kV) (T_3 , delay relative to ion trap unloading pulse); (6) mass gate switch pulse (T_4 , delay relative to ion extraction pulse); (7) momentum deceleration pulse (T_5 , delay relative to mass gate pulse); and (8) photodetachment laser on pulse (T_6 , delay relative to anion deceleration pulse). A photodiode signal from the detachment laser beam is the starting pulse for data acquisition of photoelectron time of flight.

TD500, Stanford Research Systems), which is interfaced to the PC and a display oscilloscope.

For PES experiments, the mass gate and momentum decelerator are switched on. The middle electrode of the three-grid mass gate is biased at -1300 V. Just before the arrival of the anions of interest, the mass gate high voltage is pulsed to ground potential, allowing the anions of interest to pass unaffected while stopping all other ions. The timing of the mass gate switch is referenced to the repeller pulse and the delay time (T_4) depends on the mass of the anions. Exiting the mass gate, the mass-selected anions enter the momentum decelerator. After a short delay (T_5), a +3000 V high-voltage pulse is applied across the deceleration region consisting of a series of 11 electrodes. The pulse width is determined by the mass of the anions and the amount of deceleration desired. The key of the momentum deceleration

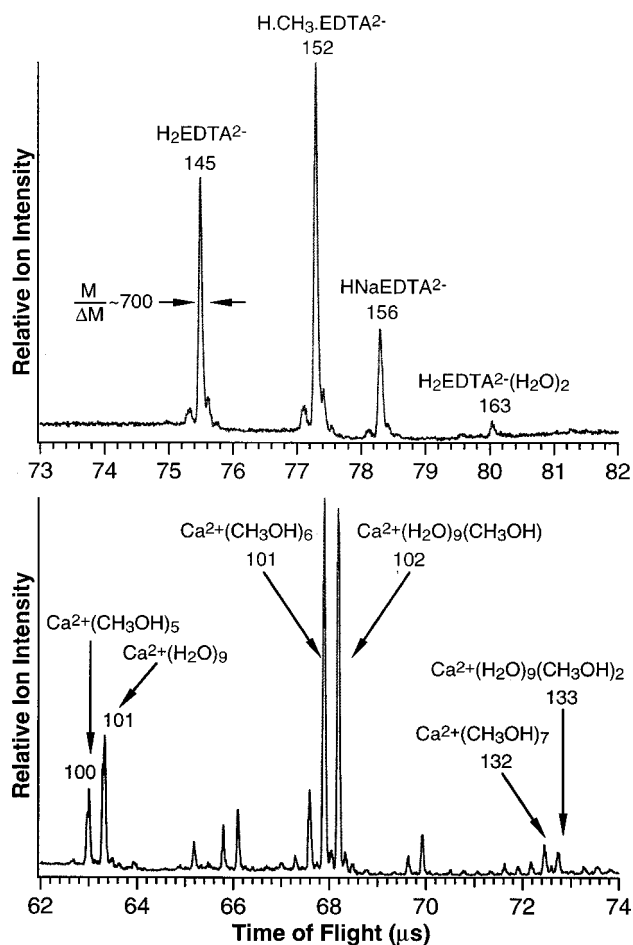


FIG. 5. Top panel: time-of-flight mass spectrum of doubly charged anions of EDTA (ethylenediaminetetraacetate) from electro spray of a 10^{-4} M EDTA sodium salt solution in a methanol/water (98/2) mixed solvent at $pH \sim 10$. The strongest peak is an ester due to reactions between EDTA and methanol. The mass resolution of about 700 is indicated. Bottom panel: time-of-flight mass spectrum of doubly charged cations from electro spray of a 10^{-4} M $CaCl_2$ solution in a methanol/water (98/2) mixed solvent at about neutral pH . The strongest peak is $Ca^{2+}(CH_3OH)_6$. Other Ca^{2+} -methanol and Ca^{2+} -methanol/water mixed complexes were also observed. The numbers indicate the M/Z of the identified peaks.

is to let the anions enter and exit the deceleration zone in a field-free condition such that all the ions experience the same deceleration field for exactly the same period of time. When the decelerated anions arrive in front of the permanent magnet tip (after a delay time, T_6), they are crossed with a detachment laser beam. The photoelectrons are collected by the magnetic bottle at nearly 100% efficiency down to the 4 m long electron flight tube, where a 10 G homogeneous magnetic field guides the electrons to the fast z -stack detector. A photodiode signal from the detachment laser pulse triggers a transient digitizer, which digitizes about 20 μ s after receiving the photodiode trigger. The registered events per laser shot are transferred to the PC where a predetermined number of laser shots are averaged.

B. TOF mass spectroscopy

Figure 5 shows two mass spectra of doubly charged anions and cations, respectively. The top panel is from electro spray of a 10^{-4} M EDTA sodium salt solution at $pH \sim 10$,

showing dianions of EDTA with two protons, one proton and a methyl group, one proton and one sodium ion, and a weak water-solvated EDTA with two protons. As indicated in Fig. 5, the mass resolution ($M/\Delta M$) was about 700, which was sufficient to resolve the ^{13}C isotopes with the expected half M/Z separations. The broad feature in front of each strong peak is an artifact due to secondary electrons from a grid right in front of the mass detector. This artifact is unique to detecting anions when a grid is used in front of the MCP detector. It does not exist in the positive ion mode (lower panel, Fig. 5), where any secondary electrons from the grid will be repelled away from the detector. Our observed resolution was consistent with our SIMION simulations. There are two key factors affecting the mass resolution. The first is the kinetic energy of the ions exiting the ion trap, i.e., the transverse kinetic energy in the TOFMS. The smaller this energy the better the resolution—ions with a smaller transverse energy can maintain more straight trajectories and do not need to be deflected much. In fact, our TOF extraction stack is mounted slightly off center (Fig. 1) to give room for the transverse motion of the ions. The second factor is the size of the ion beam in the extraction zone. The smaller the size in the perpendicular direction to the ion extraction the better the resolution. The ion packet in the trap has a dimension of about 3 mm, which will spread out in the beam direction along the way to the TOF extraction zone due to the initial ion energy spread. With our current parameters, the nominal kinetic energy is about 10 eV with a spread of at least 3–6 eV, giving a spread of the beam size slightly less than 2 cm in the extraction zone. Therefore, the 10 cm aperture of our TOF extraction stack is not the limiting factor on the mass resolution.

The bottom panel of Fig. 5 shows the doubly charged cations from electrospray of a 10^{-4} M CaCl_2 solution in a methanol/water (98/2 ratio) solution at roughly neutral pH. The spectrum shows two main series of doubly charged cations consisting of $\text{Ca}^{+2}\text{-CH}_3\text{OH}$ complexes and $\text{Ca}^{+2}\text{-CH}_3\text{OH-H}_2\text{O}$ mixed complexes at a mass resolution of about 700. The complexes containing more than nine H_2O molecules were surprising, considering the low concentration of H_2O in the solvent. However, the latter result was not yet confirmed. In any case, this experiment demonstrated that we can produce multiply charged cations as readily as the anions simply by reversing the polarities of all the electrodes in our apparatus.

The best resolution we have observed was about 800 for a low-mass singly charged anion. The resolution could be improved to about 2000 without using a reflectron either by reducing the energy and energy spread of the unloaded ion beams from the trap or by installing a smaller aperture in the TOFMS extraction stack to limit the size of the ion beams. By placing a laser-ablation target at the entrance of the TOFMS extraction stack, we have obtained a resolution of about 1500 for Cu^+ from ablation of a copper target.

However, we have observed that our mass resolution deteriorates significantly at high masses. We tested the mass resolution by spraying a protein sample, insulin chain A (IA) that has a molecular weight of 2531.6 amu. We observed three main mass peaks at $M/Z \sim 1266$, 844, and 633, corre-

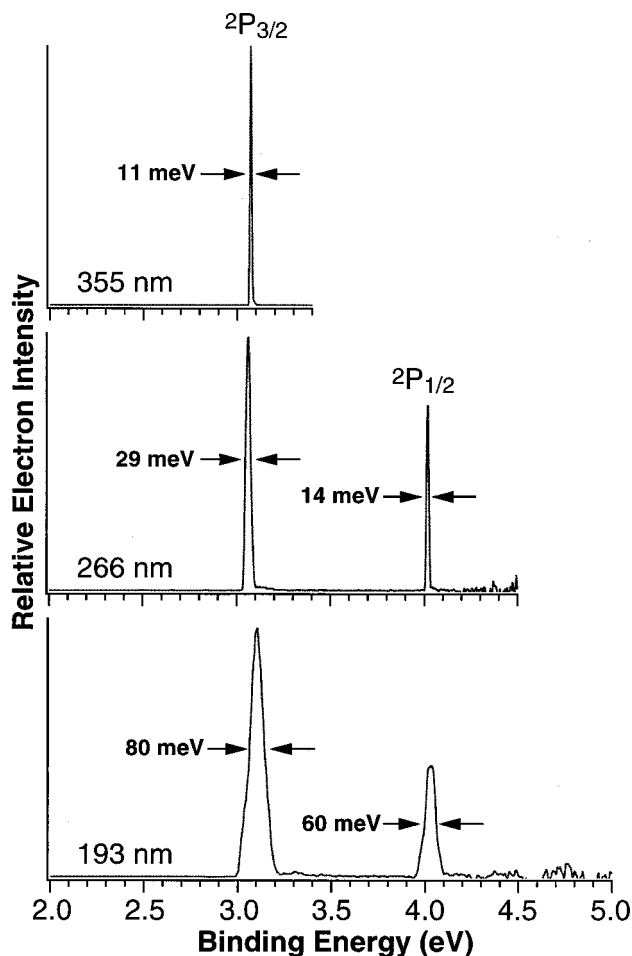


FIG. 6. Photoelectron spectra of I^- at three photon energies: 355 (3.496 eV), 266 (4.661 eV), and 193 nm (6.424 eV), showing the electron energy resolution of the new magnetic-bottle photoelectron facility and its kinetic energy dependence. The overall electron energy resolution is about $\Delta E/E = 2\%$.

sponding to IA^{-2} , IA^{-3} , and IA^{-4} , respectively. However, the mass resolution was only about 200. This mass resolution deterioration was caused by collision effects due to the high working pressure (2×10^{-5} Torr) in the TOFMS extraction chamber. It has been shown that for large molecules even a pressure of 2×10^{-6} Torr could still give a considerable collisional broadening due to the high collision cross sections of these species.⁵⁵ We have briefly tested and confirmed the collisional broadening effects. Using better differential pumping and smaller skimmers in the ion source section should improve the performance of the TOFMS at high masses.

C. Magnetic-bottle photoelectron spectroscopy

Extensive tests of the new magnetic-bottle photoelectron analyzer have been carried out. Figure 6 shows the PES spectra of I^- at three photon energies, demonstrating the resolution of the apparatus. The I^- PES spectra are routinely used to calibrate the spectrometer energy scale. The resolution of the magnetic-bottle device is strongly dependent on the initial kinetic energies of the anions, which give rise to a Doppler broadening. With the momentum decelerator, we

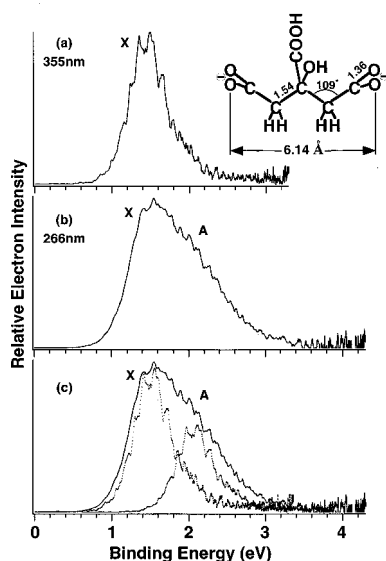


FIG. 7. Photoelectron spectra of citrate acid dianion (structure as shown) at (a) 355 nm (3.496 eV) and (b) 266 nm (4.661 eV). The additional feature observed at 266 nm is shown more clearly in (c), where two copies of the 355 nm spectrum are overlaid onto the 266 nm spectrum (see Ref. 68 for details).

can decelerate the anions down to very low kinetic energies so that the Doppler broadening is no longer the limiting factor. The resolution of the current apparatus is limited by the magnetic-field strength (500–800 G) in the detachment zone due to the simple bottle design with a single permanent magnet. We found that with our current configuration the energy resolution (FWHM) is approximately linearly proportional to the kinetic energy with $\Delta E/E \sim 2\%$. At 193 nm (ArF excimer laser), the bandwidth of the 193 nm lasing line (± 0.4 nm, ~ 30 meV FWHM) becomes a significant broadening factor.

Figure 7 shows our first PES spectra of a doubly charged anion, that of citrate dianion at 355 (3.49 eV) and 266 nm (4.66 eV). The 355 nm spectrum revealed one partially vibrationally resolved band (X). An extra band (A) was also observed in the 266 nm spectrum whereas it was absent from the 355 nm spectrum even though the photon energy was higher than the binding energies of the A band. Experiments were also performed at 532 nm (2.33 eV), but no photoelectron signals were observed even though this photon energy was higher than the binding energies of the X band. These experiments were the first to directly reveal the repulsive Coulomb barriers that bind excess electrons in multiply charged anions.⁶⁸ We have also performed a series of experiments on dicarboxyate dianions, where the separation of the two excess charges can be systematically varied.⁶⁹ Those data allowed us to determine how the excess electron binding energies and the repulsive Coulomb barriers depend on the charge separations. We have also conducted a preliminary study on water-solvated doubly charged anions to understand how solvents stabilize the excess charges.⁷⁰

V. DISCUSSION AND PERSPECTIVE

We have developed a unique and versatile experimental facility to investigate the chemistry and physics of multiply

charged anions in the gas phase. This facility will provide new research opportunities to investigate not only multiply charged anions, but also many other novel solution phase species (organic, inorganic, and biomolecular species) in the gas phase. Several improvements could still be made to further increase the performance of the apparatus. First, the mass resolution for heavy species, of major interest for biomolecules, can be increased with better vacuum in the TOFMS ion extraction zone. More importantly, the ion trap performance can be further improved. At the current configuration, no differential pumping is provided for the ion trap. Therefore, the dependence of the trapping efficiency and temperature on the background gas cannot be investigated in detail. A differential pumping system is being added to the ion trap, and will allow us not only to investigate these effects, but also to further find ways to cool the trapped ions.

ACKNOWLEDGMENTS

The authors are much indebted to Dr. Steve Hofstедler and Dr. L. Pasa-Tolic for their advice in the design of the electrospray ionization source and the quadrupole ion guide. The authors are grateful to Dr. John Price, Ken Swanson, and Jim Follansbee for their critical help in the electronics and data acquisition system. The authors also like to thank valuable discussions with Dr. S. D. Colson, Dr. Mike L. Alexander, Dr. Jeff Mack, and Professor H. Hill during the course of this work. This project is primarily supported by The U.S. Department of Energy, Office of Basic Sciences, Chemical Science Division. One of the authors (L.S.W.) would like to acknowledge Washington State University, College of Sciences, and the Alfred P. Sloan Foundation for partial support of the project. Acknowledgment is also made to the Donors of the Petroleum Research Fund; administered by the American Chemical Society, for partial support of this research. Pacific Northwest National Laboratory is operated by Battelle for the DOE under Contract No. DE-AC06-76RLO 1830. One of the authors (L.S.W.) is an Alfred P. Sloan Research Fellow.

- ¹J. W. Rabalais, *Principles of Ultraviolet Photoelectron Spectroscopy* (Wiley, New York, 1977); D. W. Turner, C. Baker, A. D. Baker, and C. R. Bundle, *Molecular Photoelectron Spectroscopy* (Wiley, New York, 1970).
- ²S. Hufner, *Photoelectron Spectroscopy—Principles and Applications* (Springer, New York, 1995).
- ³H. Hotop and W. C. Lineberger, *J. Phys. Chem. Ref. Data* **14**, 731 (1985).
- ⁴D. G. Leopold and W. C. Lineberger, *J. Chem. Phys.* **85**, 51 (1986).
- ⁵K. M. McHugh, J. G. Eaton, G. H. Lee, H. W. Sarkas, L. H. Kidder, J. T. Snodgrass, M. R. Manaa, and K. H. Bowen, *J. Chem. Phys.* **91**, 3792 (1989).
- ⁶L. S. Wang, H. S. Cheng, and J. Fan, *J. Chem. Phys.* **102**, 9480 (1995).
- ⁷S. M. Casey and D. G. Leopold, *J. Phys. Chem.* **97**, 816 (1993).
- ⁸S. H. Yang, C. L. Pettiette, J. Conceicao, O. Cheshnovsky, and R. E. Smalley, *Chem. Phys. Lett.* **139**, 233 (1987).
- ⁹G. Gantefor, K. H. Meiwes-Broer, and H. O. Lutz, *Phys. Rev. A* **37**, 2716 (1988).
- ¹⁰T. N. Kitsopoulos, C. J. Chick, Y. Zhao, and D. M. Neumark, *J. Chem. Phys.* **95**, 1441 (1991).
- ¹¹R. N. Compton, in *Photophysics and Photochemistry in the Vacuum Ultraviolet*, edited by S. P. McGlynn *et al.* (Reidel, Dordrecht, 1985).
- ¹²R. N. Compton, in *Negative Ions*, edited by V. Esaulov (Cambridge University Press, Cambridge, 1996).
- ¹³D. M. Wetzel and J. I. Brauman, *Chem. Rev.* **87**, 607 (1987).
- ¹⁴J. Kalcher and A. F. Sax, *Chem. Rev.* **94**, 2291 (1994).

- ¹⁵M. K. Scheller, R. N. Compton, and L. S. Cederbaum, *Science* **270**, 1160 (1995).
- ¹⁶G. R. Freeman and N. H. March, *J. Phys. Chem.* **100**, 4331 (1996).
- ¹⁷L. L. Mack, P. Kralik, A. Rheude, and M. Dole, *J. Chem. Phys.* **52**, 4977 (1970).
- ¹⁸M. Yamashita and J. B. Fenn, *J. Phys. Chem.* **88**, 4451,4671 (1984).
- ¹⁹J. Fenn, M. Mann, C. K. Meng, S. F. Wong, and C. M. Whitehouse, *Science* **246**, 64 (1989).
- ²⁰*Biochemical and Biotechnological Applications of Electrospray Ionization Mass Spectrometry*, edited by A. P. Snyder (ACS, Washington, DC, 1995).
- ²¹T. C. Lau, J. Wang, K. W. M. Siu, and R. Guevremont, *J. Chem. Soc. Chem. Commun.* 1487 (1994).
- ²²T. C. Lau, J. Wang, R. Guevremont, and K. W. M. Siu, *J. Chem. Soc. Chem. Commun.* 877 (1995).
- ²³A. T. Blades and P. Kebarle, *J. Am. Chem. Soc.* **116**, 10761 (1994).
- ²⁴A. T. Blades, J. S. Klassen, and P. Kebarle, *J. Am. Chem. Soc.* **117**, 10563 (1995).
- ²⁵J. S. Klassen, A. T. Blades, and P. Kebarle, *J. Phys. Chem.* **99**, 15509 (1995).
- ²⁶R. C. Dougherty, *J. Chem. Phys.* **50**, 1896 (1969).
- ²⁷J. H. Bowie and B. J. Stapleton, *J. Am. Chem. Soc.* **98**, 6480 (1976).
- ²⁸A. P. Bruins, T. R. Covey, and J. D. Henion, *Anal. Chem.* **59**, 2642 (1987).
- ²⁹L. O. G. Weidolf, E. D. Lee, and J. D. Henion, *Biomed. Environ. Mass Spectrom.* **15**, 283 (1988).
- ³⁰W. P. M. Maas and N. M. M. Nibbering, *Int. J. Mass Spectrom. Ion Processes* **88**, 257 (1989).
- ³¹S. N. Schauer, P. Williams, and R. N. Compton, *Phys. Rev. Lett.* **65**, 625 (1990).
- ³²D. Calabrese, A. M. Covington, and J. S. Thompson, *J. Chem. Phys.* **105**, 2936 (1996).
- ³³D. Mathur, V. R. Bhardwaj, F. A. Rajgara, and C. P. Safvan, *Chem. Phys. Lett.* **277**, 558 (1997).
- ³⁴R. L. Hettich, R. N. Compton, and R. H. Rotchie, *Phys. Rev. Lett.* **67**, 1242 (1991).
- ³⁵P. A. Limbach, L. Schweikhard, K. A. Cowen, M. T. McDermott, A. G. Marshall, and J. V. Coe, *J. Am. Chem. Soc.* **113**, 6795 (1991).
- ³⁶C. Jin, R. L. Hettich, R. N. Compton, A. Tuinman, A. Derecskei-Kovacs, D. S. Marynick, and B. I. Dunlap, *Phys. Rev. Lett.* **73**, 2821 (1994).
- ³⁷R. N. Compton, A. A. Tuinman, C. E. Klots, M. R. Pederson, and D. C. Patton, *Phys. Rev. Lett.* **78**, 4367 (1997).
- ³⁸G. Khairallah and J. B. Peel, *J. Phys. Chem. A* **101**, 6770 (1997).
- ³⁹O. V. Boltalina, P. Hvelplund, M. C. Larsen, and M. O. Larsson, *Phys. Rev. Lett.* **80**, 5101 (1998).
- ⁴⁰E. V. Stefanovich, A. I. Boldyrev, T. N. Truong, and J. Simons, *J. Phys. Chem. B* **102**, 4205 (1998).
- ⁴¹V. Berghof, T. Sommerfeld, and L. S. Cederbaum, *J. Phys. Chem. A* **102**, 5100 (1998).
- ⁴²A. I. Boldyrev, M. Gutowski, and J. Simons, *Acc. Chem. Res.* **29**, 497 (1996).
- ⁴³T. Sommerfeld, M. K. Scheller, and L. S. Cederbaum, *J. Chem. Phys.* **104**, 1464 (1996).
- ⁴⁴M. K. Scheller and L. S. Cederbaum, *Chem. Phys. Lett.* **216**, 141 (1993).
- ⁴⁵M. K. Scheller and L. S. Cederbaum, *J. Chem. Phys.* **100**, 8943 (1994).
- ⁴⁶L. S. Wang, J. Conceicao, C. Jin, and R. E. Smalley, *Chem. Phys. Lett.* **182**, 5 (1991).
- ⁴⁷P. Kruit and F. H. Read, *J. Phys. E* **16**, 313 (1983).
- ⁴⁸O. Cheshnovsky, S. H. Yang, C. L. Pettiette, M. J. Craycraft, and R. E. Smalley, *Rev. Sci. Instrum.* **58**, 2131 (1987).
- ⁴⁹H. Handschuh, G. Gantefor, and W. Eberhardt, *Rev. Sci. Instrum.* **66**, 3838 (1995).
- ⁵⁰L. S. Wang and H. Wu, in *Advances in Metal and Semiconductor Clusters, IV, Cluster Materials*, edited by M. A. Duncan (JAI, Greenwich, 1997).
- ⁵¹J. G. Boyle, C. M. Whitehouse, and J. B. Fenn, *Rapid Commun. Mass Spectrom.* **5**, 400 (1991).
- ⁵²J. G. Boyle and C. M. Whitehouse, *Anal. Chem.* **64**, 2084 (1992).
- ⁵³O. A. Mirgorodskaya, A. A. Shevchenko, I. V. Chernushevich, A. F. Dodonov, and A. I. Miroshnikov, *Anal. Chem.* **66**, 99 (1994).
- ⁵⁴A. N. Verentchikov, W. Ens, and K. G. Standing, *Anal. Chem.* **66**, 126 (1994).
- ⁵⁵I. V. Chernushevich, A. N. Verentchikov, and K. G. Standing, *J. Am. Soc. Mass Spectrom.* **7**, 342 (1996).
- ⁵⁶J. K. Olthoff, I. A. Lys, and R. J. Cotter, *Rapid Commun. Mass Spectrom.* **2**, 171 (1988).
- ⁵⁷J. H. J. Dawson and M. Guilhaus, *Rapid Commun. Mass Spectrom.* **3**, 155 (1989).
- ⁵⁸*Practical Aspects of Ion Trap Mass Spectrometry*, edited by R. E. March and J. F. J. Todd Vol. I–III (CRC, New York, 1995), Vols. I–III.
- ⁵⁹S. T. Fountain, H. Lee, and D. M. Lubman, *Rapid Commun. Mass Spectrom.* **8**, 487 (1994).
- ⁶⁰B. M. Chien, S. M. Michael, and D. M. Lubman, *Int. J. Mass Spectrom. Ion Processes* **131**, 149 (1994).
- ⁶¹R. W. Purves and L. Li, *J. Am. Soc. Mass Spectrom.* **8**, 1085 (1997).
- ⁶²D. M. Chambers, L. I. Grace, and B. D. Andresen, *Anal. Chem.* **69**, 3780 (1997).
- ⁶³P. Grant, D. Chambers, L. Grace, D. Phinney, and I. Hutcheon, *Phys. Today* **32**, 51 (1998).
- ⁶⁴M. Busman, A. L. Rockwood, and R. D. Smith, *J. Phys. Chem.* **96**, 2397 (1992).
- ⁶⁵D. J. Douglas and J. B. French, *J. Am. Soc. Mass Spectrom.* **3**, 398 (1992).
- ⁶⁶W. C. Wiley and I. H. McLaren, *Rev. Sci. Instrum.* **26**, 1150 (1955).
- ⁶⁷W. A. de Heer and P. Milani, *Rev. Sci. Instrum.* **62**, 670 (1991).
- ⁶⁸X. B. Wang, C. F. Ding, and L. S. Wang, *Phys. Rev. Lett.* **81**, 3351 (1998).
- ⁶⁹L. S. Wang, C. F. Ding, X. B. Wang, and J. B. Nicholas, *Phys. Rev. Lett.* **81**, 2667 (1998).
- ⁷⁰C. F. Ding, X. B. Wang, and L. S. Wang, *J. Phys. Chem.* **102**, 8633 (1998).